

# Pulsed-DC Reactive Sputtering of Dielectrics: Pulsing Parameter Effects

A. Belkind and Z. Zhao, Stevens Institute of Technology, Hoboken, NJ;  
and D. Carter, L. Mahoney, G. McDonough, G. Roche, R. Scholl and H. Walde,  
Advanced Energy Industries, Inc., Fort Collins, CO

**Key Words:** Pulsed deposition  
Pulsed plasma

Reactive sputtering  
 $\text{Al}_2\text{O}_3$

## ABSTRACT

Pulsed DC power is used for reactive sputtering of dielectrics. At certain pulsing frequencies and duty cycles, deposition can be done without arcing and high deposition rates can be achieved. In this work, the influence of frequency, on-time and off-time durations on the deposition process are investigated.

## I. INTRODUCTION

DC reactive sputtering of dielectrics is often accompanied with strong arcing. Arcing appears mainly on the portion of the target surface that is not strongly bombarded by positive ions and may therefore be covered with a dielectric layer. Such a dielectric layer accumulates positive charges, which if dense enough, may cause arcing. To avoid this arcing, reactive sputter-deposition of dielectric films is done using either pulsed-DC [1-14] or mid-frequency ac power [15-17]. Pulsed-DC power is implemented mainly with a single magnetron system, while ac power is generally used with a dual magnetron arrangement. A waveform showing the effect of pulsed-DC power is shown in Figure 1. The pulsing parameters must satisfy certain conditions to avoid arcing. These conditions are usually satisfied when pulsing frequencies and duty cycle (defined as the ratio  $\tau_{on}/(\tau_{on} + \tau_{off})$ ) are chosen properly from the range of about 20-350 kHz and 0.5-0.9, respectively. Pulsing parameters such as duty cycle and off-time influence also the forms of voltage and current peaks, deposition rate and the properties of the deposited thin films. In this paper, the proper choice of pulsing frequency and some details of pulsing parameter influences are described. Results are given for pulsed dc reactive sputtering of  $\text{Al}_2\text{O}_3$  thin film.

## 2. EXPERIMENTAL TECHNIQUE

The experiments were done in a box coater with a planar rectangular unbalanced magnetron HRC-817 (BOC Coating Technology) previously described in [11,13,14]. The pulsed DC power was applied to the cathode using a DC power supply, model MDX-10 by Advanced Energy Industries (AEI), pulsed generator Sparcle<sup>®</sup>-V (AEI), and also by a PinnaclePlus<sup>®</sup> unit (AEI). The DC power supply was run in the constant power and current modes. Another model of pulsed power supply, RPG (ENI), was used for comparison.

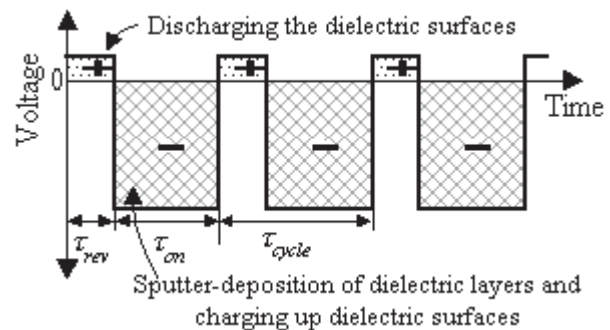


Figure 1. Pulsed voltage used to power a cathode

The current and voltage pulse forms were recorded using an oscilloscope model TDS 340, connected to a voltage probe model P5100, and a current probe, model A6303, (all from Tektronix). The pulsed power consumed by the plasma was obtained by dynamic multiplication (point-by-point) of the current and voltage waveforms. Plasma emission was recorded by two photomultipliers H5783 (Hamamatsu) with narrow filters attached to each of them to record  $\text{Ar}^+$  (425 nm) and atomic oxygen (777 nm) emission. The time constant of optical responses was less than 10 ns.

## 3. PULSING PARAMETERS AND CATHODE MICROARCING

It is commonly accepted that positive charges accumulated on the surface of a dielectric layer deposited (or grown) on the target surface, are the main source of arcs. Accumulation of these charges takes place during each on-time pulse,  $\tau_{on}$  (Figure 1) as ions bombard the target surface. During the following off-time,  $\tau_{off}$ , electrons from the residual plasma discharge the layer. If the discharge is not complete, additional step-by-step charge accumulation during many sequential periods takes place, and layer breakdown may still occur. Let us consider first only charge accumulation in a single on-time.

If the electrical field in the dielectric layer created by the charge accumulated during an on-period exceeds the dielectric strength of the film, a breakthrough takes place in the film, and, as a result of a high level of electron emission from the

breakthrough area, an arc appears. Estimations have been made [2,3,13,14,18] which show that, at the deposition conditions used in typical cases, a breakdown field of  $E_{br} \approx 10^6$  V/cm appears in the  $Al_2O_3$  films in about  $\tau_{br} = 0.1$ -1 ms. To avoid such arcs, the on-time,  $\tau_{on}$ , (Figure 1) should not larger than 0.1-1 ms and the pulsing frequency should be larger than the related critical frequency  $f_{cr,1} = 1$ -10 kHz.

Another kind of microarc can appear when a high electrical field is created between positive charges accumulated on the dielectric layer and a nearby open metal surface of the race-track area. These might be called surface creepage breakdown. The traces of these microarcs are seen on the target surface as scratches. Very little is known about their electrical parameters. To avoid this kind of arcing, the on-time should not be larger than some duration dependent upon surface conditions; that is to say, the pulsing frequency should be larger than a critical frequency,  $f_{cr,2}$ . So, to avoid microarcing due to charge accumulation in a single on-time pulse, the on-time should less than a certain value, which is to say that the frequency should be larger than  $f_{cr,1}$  or  $f_{cr,2}$ , whichever is higher. It is important to note that that  $f_{cr,1}$  or  $f_{cr,2}$  do not depend on the duty cycle, because they relate to an arc formed by charge buildup in a single on-time period.

Another limitation for pulsing frequency comes from possible step-by-step charge accumulation during many sequential periods. To avoid such accumulation, the dielectric surfaces must be discharged completely during each off-time,  $\tau_{off}$  (also called the "reverse time",  $\tau_{rev}$ ). For this to occur, for each period  $\tau_{on}$ , a minimal  $\tau_{off,min}$  exists to avoid arcing. It is obtained as a first approximation that  $\tau_{off,min}$  is linearly related to  $\tau_{on}$ , and the relationship coefficient is directly proportional to the current [13,14]. The linear relationship between these durations leads to a simple upper limitation on the duty cycle,  $d_{cr}$ , which decreases as the current increases.

Experimentally, the conditions for avoiding microarcs may be verified by counting microarcs at different pulsing frequencies. This may be done keeping on-time, off-time, or duty cycle, constant. The number of microarcs counted in a certain time is usually very low until the frequency is decreased to the critical frequency  $f_{cr}$ . Continuous arcing is observed at  $f_{cr}$  and lower [11,13,14]. In accordance with the discussed conditions, to avoid arcing and experimental data, the critical frequency depends on the duty as shown in Figure 2.

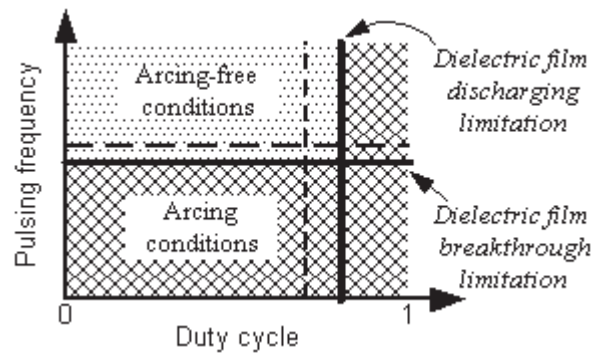


Figure 2. First-approximation view of arcing-free conditions in the 2-d space of pulsing frequency and duty cycle and two different currents,  $I_1$  (solid lines) and  $I_2$  (dotted lines):  $I_1 < I_2$ .

#### 4. PULSING PARAMETERS AND DISCHARGE BEHAVIOUR

Current and voltage pulses during reactive sputtering of a dielectric are shown schematically in Figure 3. An example of actual shapes of current and voltage pulses as well as optical emission pulses, is shown Figure 4 [11,13,14]. Let us consider a moment when the cathode voltage is switched to a positive value (Point A on the time scale, Figure 3). Since at this moment the plasma support is turned off, the plasma begins to decay through bipolar charge carrier diffusion to the wall of the chamber, and the electrodes. As the plasma density diminishes, the electron current to the positive target decreases. As may be seen in Figure 3, the shape of the electron current waveform between times A and B may be described by two exponentials, with time constants of  $\tau_{est,1} = 30 \div 40 \mu s$  and  $\tau_{est,2} = 3 \div 5$  ms for the balanced magnetron and of  $\tau_{est,1} \approx 15 \mu s$  for the unbalanced magnetron [13,14]. The longest time constant is consistent with the overall plasma decay. These time constants are close to those observed in various high-density oxygen plasmas [19]. The larger time constant is consistent with Bohm bipolar plasma diffusion to the walls [20]. Note that the plasma emission in pulsed power reactive sputtering of  $Al_2O_3$  recorded for the Al-line and O-line, also decay, but not at the same rate; to a first approximation, the emission lines decay exponentially with two time constants:  $0.2$ - $0.3 \mu s$  and  $1 \mu s$ . This may be explained by noting that the excitation of optical emission in the plasma requires involvement of electrons with energies above about 10 eV. It is to be expected that when the plasma starts to decay, the fast electrons disappear much faster the slow ones [20]. Although the time constants obtained for optical emission are less than the ones obtained for electron current decay, they still confirm that there is a substantial plasma density at the end of a few microsecond-long off-time.

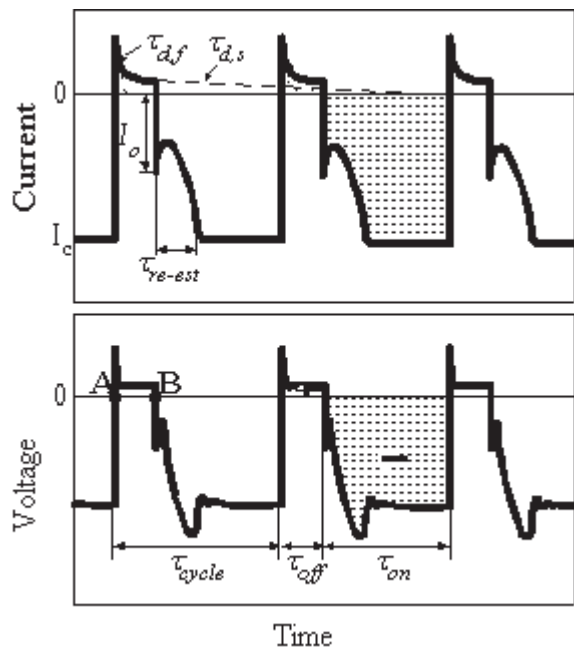


Figure 3. Typical current and voltage oscillograms

So, if the  $\tau_{off}$  is of an order of a few microseconds or less, then at this moment a plasma still exists in the space between the cathode and anode, although its density has fallen off. The density of this residual plasma,  $n_{e,res}$  depends on the off-time,  $\tau_{off}$ ; increasing  $\tau_{off}$  decreases the density  $n_{e,res}$ .

The negative voltage is turned on again at the end of the off-, or reverse-, time (Point B on the time scale, Figure 3). At this moment, the density  $n_{e,res}$  determines the initial current,  $I_o$ , and also the re-establishment time,  $t_{re-est}$  (Figure 3). The higher the residual concentration of charge carriers  $n_{e,res}$  (i.e., the smaller the off-time), the larger the current  $I_o$  and lower the duration  $\tau_{re-est}$ .

Plasma re-establishment time depends on the residual plasma density  $n_{e,res}$ , which increases with increasing cathode current and decreasing off-time. It takes, usually, a  $\tau_{re-est} = 1-2 \mu s$ , sometimes even less, to recover to the original density. Such fast plasma re-establishment is promoted by a voltage overshoot created by the dc power supply, which will occur if the power supply has any substantial output inductance.

The unbalanced magnetron plasma decay time constants are higher than those of the balanced magnetron. This could be related to the fact that the dense part of the unbalanced magnetron plasma occupies much larger volume, and its decay thus requires a longer time.

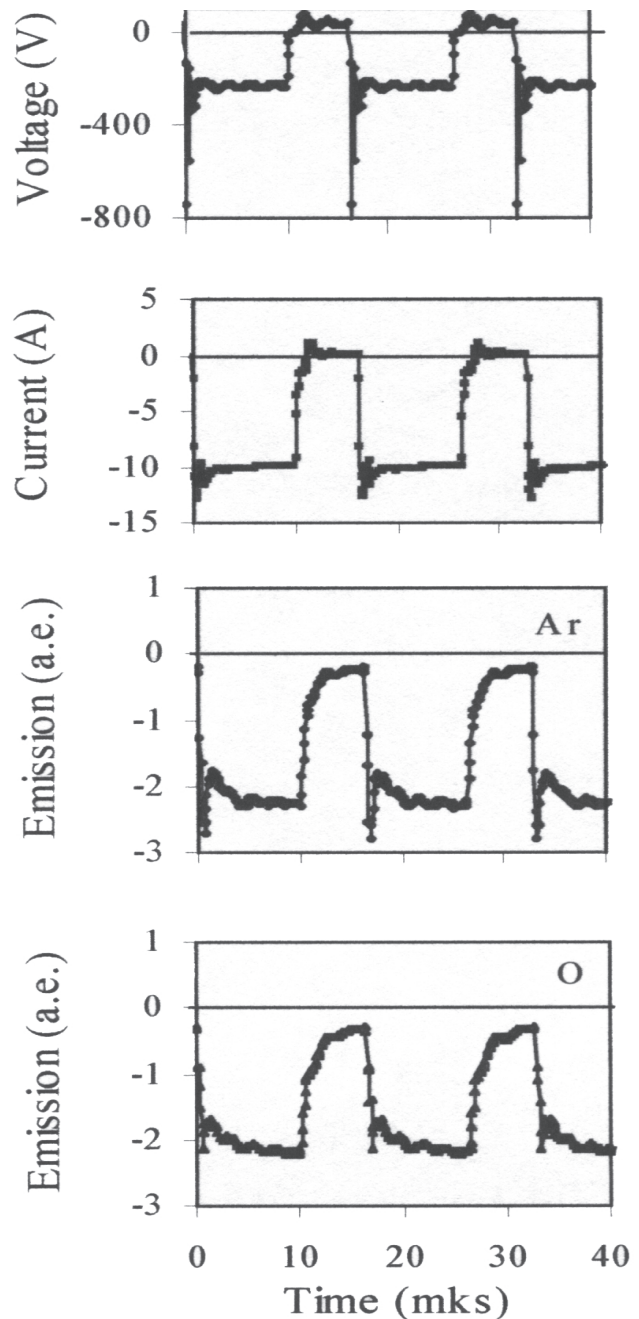


Figure 4. Voltage, current, and optical emission of Ar and O oscillograms.

## 5. PULSING PARAMETERS AND TARGET STATE OF OXIDATION

The target surface in the racetrack area of a magnetron in reactive sputtering can be in either of two stable states or modes: metallic and reactive. If the target is largely or completely covered with oxide, it is said that the system is operating in the "oxide mode". In the "metallic mode", the racetrack area is practically clean from oxide, and sputtering of the metal is the dominant process. In addition to these stable

modes, the target racetrack area can be maintained also in an intermediate mode, which is not ordinarily stable, by employing a closed-loop control system. In all cases, the balance of sputtering and oxidation rates determines the racetrack area's surface conditions. Sputtering takes place only during the on-time, while oxidation takes place in both parts of the cycle, during the off-time as well as the on-time. During the on-time, oxidation takes place mainly by atomic oxygen generated in the plasma. During the off-time, oxidation is provided by the decaying concentration of atomic oxygen that at the end of an off-time is still high (emission of atomic oxygen line is still strong).

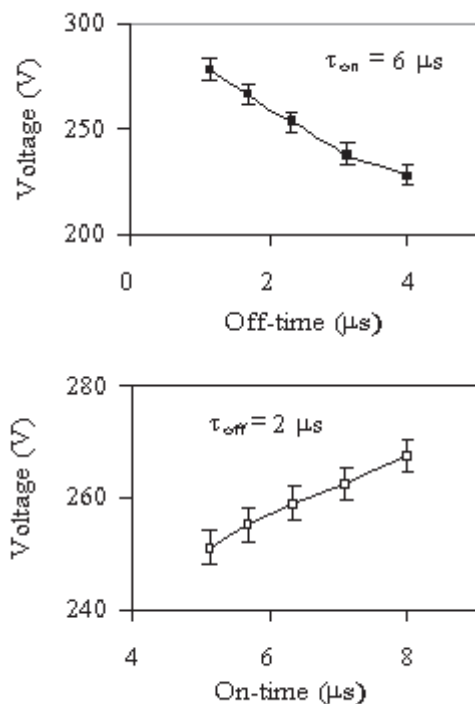


Figure 5. Voltage versus off-time at constant on time (upper) and versus on-time at constant off-time (lower).

Changing the duty cycle will change the equilibrium between oxidation and sputtering processes and result in a different average thickness of the oxide layer on the target surface. It is worthwhile to notice that the thickness of the oxide layer, even in the oxide mode, is very small; if this were not true, a substantial voltage drop would build up due to charging of the oxide layer, which would cut off the discharge. In spite of being very thin, however, slightly different thickness in the oxide layer leads to variation of the cathode voltage and deposition rate. An effect related to the target oxidation state is actually seen in the variation of the cathode voltage as shown in Figure 5. It is also seen in a variation of the linear relationship between the deposition rate and power consumed in the plasma at different constant duty cycles (Figure 6).

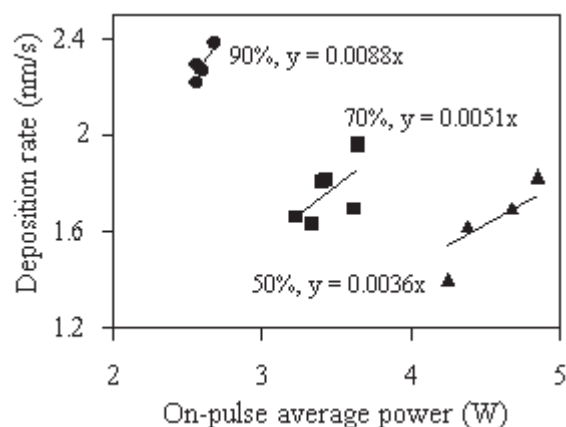


Figure 6. Deposition rate versus on-pulse average power at different constant duty cycles.

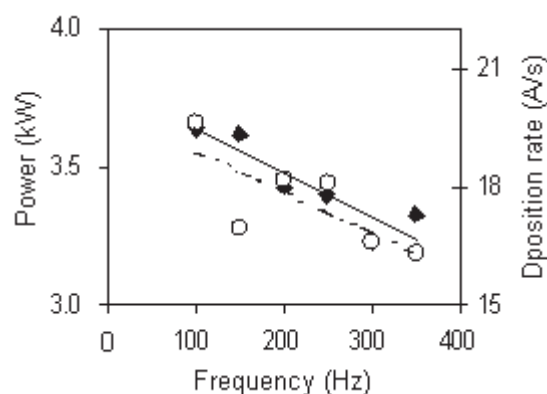


Figure 7. On-pulse average power (closed diamonds) and deposition rate (open circles) versus frequency at constant power of 2.5 kW and 0.7 duty cycle.

## 6. PULSING PARAMETERS AND POWER DISSIPATION

The pulsed power delivered to the plasma (i.e., the power delivered during the on-time) is slightly lower than the power generated by supply (Figure 7). The difference between the two increases with frequency; this is probably due to power loss in the pulsing device (the electronic switches dissipate a little energy for each switch operation, and thereby power loss increases with frequency). Deposition rate, measured in the power supply's constant power mode, also decreases with increasing frequency (Figure 7). It has been shown [13,14] that the deposition rate in pulsed systems is directly proportional to the power delivered to the plasma during the on-time.

The power delivered to magnetron to generate the plasma is released mainly in sputtering of the target material, but also can be lost through heating all surfaces: the target, chamber walls, and substrates. The power distribution between the sputtering and other processes depends on the pulsing fre-

quency. For example, increasing the frequency increases substrate and wall heating, due to increased ion bombardment due to increased floating potential, in turn caused by increased electron temperature and plasma density at surfaces remote to the plasma.

## 7. CONCLUSION

Pulsing power is used to perform reactive sputtering of dielectrics. Its implementation has discovered various processes that influence deposition characteristics. These processes include plasma dynamics, sputtering and oxidation of the target, deposition of an oxide layer on the anode surface and its resputtering, and others. The analysis shows that:

- Reactive sputtering of dielectrics can be performed without arcing using pulsing frequencies that exceed the critical frequency, and a duty cycle that is less than the critical duty cycle.
- The critical frequency increases with the power (or current) delivered to the target.
- The critical duty cycle decreases as the target power or current increases.
- Plasma dynamics determines the kinetics of the voltage and current pulses
- Pulsing parameters (frequency and off-time) affect the principal reactive sputtering parameters: voltage, deposition rate, substrate heating, etc.
- Increasing the duty cycle at constant power provided by the power supply decreases the oxidation state of the target surface and, therefore, increases the deposition rate
- Increasing the pulsing frequency increases power loss, both in the pulser switching devices and in substrate and wall heating. As the power measured by the power supply does not include these losses, there is an *apparent* decrease in specific deposition rate (deposition rate per watt) due to a decreasing fraction of the measured power being delivered to the target. This effect disappears when the actual power delivered to the plasma is measured and used as the power figure.

## REFERENCES

1. R. Scholl, in 36th Annual Technical Conference Proceedings, Dallas (Society of Vacuum Coaters), p. 405 (1993).
2. S. Schiller, K. Goedicke, J. Reschke, V. Kirchke, S. Schneider, and F. Milde, Surf.Coat.Technol., 61, 331 (1993).
3. R. Scholl, in 37th Annual Technical Conference Proceedings, Boston (Society of Vacuum Coaters) p. 312 (1994).
4. W.D. Sproul, M.E. Graham, M.S. Wong, S. Lopez, D. Li, and R.A. Scholl, J.Vac.Sci.Technol., A 13, 1188 (1995).
5. F. Fietzke, K. Goedicke, and W. Hempel, Surf.Coat.Technol., 86-87, 657 (1996).
6. P.J. Kelly, O.A. Abu-Zeid, R.D. Arnell, and J. Tong, Surf.Coat.Technol., 86-87, 28 (1996).
7. V. Kirchoff and T. Kopte, in 39th Annual Technical Conference Proceedings, Philadelphia, PA (Society of Vacuum Coaters), p. 117 (1996).
8. J.C. Sellers, in 39th Annual Technical Conference Proceedings, Philadelphia, PA (Society of Vacuum Coaters), p. 123(1996).
9. S. Schiller, V. Kirchoff, K. Goedicke, and P. Frach, in 40th Annual Technical Conference Proceedings, New Orleans, LA (Society of Vacuum Coaters), 129(1997).
10. O. Zywitzki and G. Hoetzsch, Surf.Coat.Technol., 94-95, 303 (1997).
11. A. Belkind, A. Freilich, and R. Scholl, in 41st Annual Technical Conference Proceedings, Boston, 1998 (Society of Vacuum Coaters), p. 321 (1998).
12. J.M. Schneider and W.D. Sproul, in 98/1 Reactive Sputtering. W.D. Westwood, ed. (Institute of Physics Publishing, Bristol and Philadelphia), p. A5.1:1 (1998).
13. A. Belkind, A. Freilich, and R. Scholl, Surf.Coat.Technol., 108-109, 558 (1998).
14. A. Belkind, A. Freilich, and R. Scholl, J.Vac.Sci.Technol., A 17, 1934 (1999).
15. R.L. Cormia and T. Tumbly, US Patent 4,046,659 (Sept. 1977).
16. G. Este and W.D. Westwood, J.Vac.Sci.Technol., A 6, 1845 (1988).
17. D.A. Glocker, J.Vac.Sci.Technol., A 11, 2989 (1993).
18. J. Szczyrbowski, G. Brauer, W. Dicken, M. Scherer, W. Maas, G. Teschner, A. Zmelty, Surf.Sci.Techol., 93, 14 (1997).
19. J.P. Booth and N. Sadeghi, J.Appl.Phys., 70, 611 (1991).
20. M.A. Lieberman, Plasma Sources Sci.Technol., 5, 145 (1996).